On the lensed blazar B0218+357

R. Falomo[1]⋆ A. Treves[2], R. Scarpa[3,4] S. Paiano[1], and M. Landoni[5]

[1] *INAF – Osservatorio Astronomico di Padova, Vicolo dell'Osservatorio 5, I-35122 Padova (PD), ITALY*
[2] *Università degli Studi dell'Insubria, Via Valleggio 11 I-22100 Como - ITALY*
[3] *Instituto de Astrofisica de Canarias, C/O Via Lactea, s/n E38205 - La Laguna (Tenerife) - SPAIN*
[4] *Universidad de La Laguna, Dpto. Astrofsica, E-38206 La Laguna (Tenerife) SPAIN*
[5] *INAF, Osservatorio Astronomico di Brera, Via E. Bianchi 46 I-23807 Merate (LC) - ITALY*

5 June 2017

ABSTRACT

We present an optical spectrum ($\lambda\lambda$ 4000–10500 Å) of the lensed blazar B0218+357 secured at the 10m GTC and aimed to investigate and clarify the properties of this intriguing system. We found that the emission line spectrum of the blazar is characterised by only one broad emission line that interpreted as Mg II 2800 Å yields z = 0.95. In addition we detect narrow absorption lines of Mg II 2800 Å and Ca II (H,K) and Na I 5892 Å at z=0.68437 $\pm$ 0.00005 due to intervening interstellar gas. No stellar absorption features attributable to the lens galaxy are revealed. Thus the assumed redshift of the lens is dubious. The continuum spectrum of the object exhibits a remarkable drop towards the short wavelengths likely due to a significant extinction. This extinction cannot be produced in the lens galaxy at z =0.684 with any value of R_V under the assumption that the intrinsic shape of the blazar is dominated by a power law emission. However, the observed continuum is consistent with a power law emission assuming a standard ($R_V = 3.1$) extinction at the source redshift (z = 0.95) as supported also by the presence of Mg II absorptions at the same redshift. HST images of B0218+357 exhibit the double image of the source together with extended image of a face on spiral galaxy. We argue that this galaxy is possibly not the lensing galaxy but the host galaxy of the blazar. This has substantial consequences on the models of the system and on the derived values of the Hubble constant.

Key words: galaxies: galaxies: active — galaxies: nuclei — quasars: general

1 INTRODUCTION

B0218+35 is a real wonder of the sky. It is one of the best studied gravitational lenses with a double radio image (A+B) separated by 0.33 arcsec, and a clear example of Einstein radio ring , with a diameter similar to the above given separation (e.g. Patnaik et al. 1993; Biggs et al. 2001). A and B exhibit correlated flux variability which is relevant for the measurement of the Hubble constant (e.g. Refsdal 1964). The redshift of the lens was measured at z=0.684 (Browne et al. 1993), while for the source a redshift z = 0.94 was proposed by Browne et al. (1993) and then confirmed by Lawrence (1996) . The source is very active at high energies (e.g. Giommi et al. (2012); Cheung et al. (2014)), and it is classified as a blazar. Till now it is the farthest object detected at $\sim$1 TeV with Cherenkov telescopes (Ahnen et al. 2016).

B0218+35 was imaged several times with HST (Jackson et al. 2000; Lehár et al. 2000; Muñoz et al. 2004; York et al. 2005). The counterparts of the two radio sources are clearly detected, the brighter radio one (A) being the fainter in the optical. This is generally interpreted as due to absorption in a giant molecular cloud obscuring A, which is supposedly responsible of H I (21-cm) and other absorption lines detected in the radio band (Carilli et al. 1993). A diffuse emission which is generally associated with the lens galaxy is observed in the HST images. York et al. (2005) and references therein propose an interpretation as a spiral viewed face on.

In the course of a systematic study of spectral properties of TeV blazar sources at the GTC 10.4m telescope B0218+35 was observed by our group in 2015 (Paiano et al. (2017)). In this paper we examine in detail our spectrum and discuss it in the context of the ample literature on the optical properties of the source. The paper is organised as follows: in Section 2 we review the optical properties of the system. Section 3 deals with our spectroscopic observations and analysis. Finally in Section 4 we illustrate and discuss

⋆ E–mail:

the implications of our results. In this work we adopt the concordance cosmology with $H_0 = 70$ km s^{-1} Mpc^{-1}, $\Omega_m = 0.3$ and $\Omega_\Lambda = 0.7$.

2   REVIEW OF OPTICAL DATA OF B0218+35

The first optical spectrum of the source was obtained by Browne et al. (1993) who clearly detected absorption features of Ca II (H, K) and a very faint absorption attributed to Mg II 2800 Å of the lens galaxy at z=0.684. They also propose the detection of very weak and narrow emission lines of [OII] 3727Å and [OIII] 5007Å. In addition they suggest the presence of a weak and broad emission line at 5418 Å tentatively identified as Mg II 2800 Å at z = 0.936 and attributed to the source (the blazar). A better spectrum obtained by Lawrence (1996) confirmed the Ca II and Mg II absorptions at z=0.684 and the broad emission at $\sim$ 5400 Å with an associated absorption doublet. The redshift of the lens galaxy was confirmed through 21 cm HI absorption by Carilli et al. (1993) and through molecular gas of CO, HCO and HCN by Wiklind & Combes (1995) .

A superior quality but uncalibrated optical spectrum was obtained by Cohen et al. (2003) who confirm the above absorption features and clearly detect a strong broad emission line at 5470 Å identified as Mg II 2800 Å yielding a redshift of z = 0.944 for the blazar. In addition these authors claimed the detection of emission lines of [OII] 3727, H$_\beta$ and [OIII] at z = 0.684 thus attributed to the lens galaxy. Moreover they also suggest the presence of weak H$_\beta$ and [OIII] emission in the red noisy spectrum, attributed to the blazar at z = 0.944

HST images were obtained by Jackson et al. (2000); Lehár et al. (2000); Muñoz et al. (2004) using WFPC2 and NICMOS and by York et al. (2005) using ACS. From WFPC2 images in V and I filters Jackson et al. (2000) clearly detect the two images of the blazar separated by $\sim$ 0.3 arcsec. The separation between the two images may be less at optical and infrared wavelengths (318 $\pm$ 5 mas at near-IR Jackson et al. (2000) ; 317 $\pm$ 4 York et al. (2005)) than that derived at radio wavelengths (334 $\pm$ 1 mas Patnaik et al. 1993, unitis1995). This incited some doubts on the interpretation of B0218+35 as a lensed object. In addition to the double image HST data show a "smooth brightness" around the two sources that is attributed to the lensing galaxy. The estimated flux density of the lens galaxy is : 0.06, 0.13 and 0.15 (10^{-16} erg cm^{-2} s^{-1} Å^{-1}) in the bands F555W, F814W and F160W, respectively (Jackson et al. 2000). At the redshift of the lens (z= 0.684) these observations correspond to rest frame emission at $\lambda \sim$ 3300, 4800 and 9500 Å. The F160W observations is close to rest frame I band. Assuming the lens is a spiral galaxy (Jackson et al. 2000; York et al. 2005) the k-corrected absolute magnitude would be M$_I$ (lens galaxy) $\sim$ −23.5 (AB mag). Similar results were obtained by Lehár et al. (2000) who, in addition, performed also an image decomposition using the H band image. It turned out that the lens galaxy is described by an exponential disk with an effective radius R$_e$ = 0.19 $\pm$ 0.01 arcsec. This would yield an extremely compact galaxy since at the redshift of the lens it corresponds to only $\sim$ 1.4 kpc. The lens galaxy appears almost centred on the B source (see Figure 1). Further HST optical images were secured using WFC of ACS by York
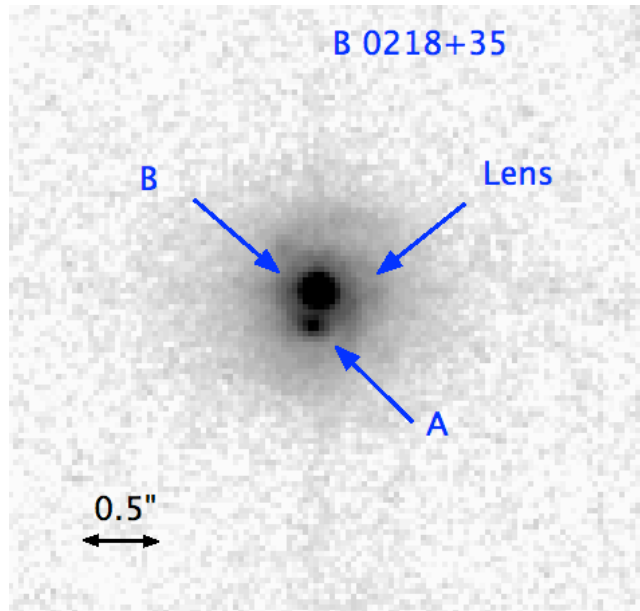

Figure 1. HST ACS WFC image of B0218+35 (filter F814W). The double point-like source is clearly detected surrounded by an extended nebulosity attributed to the lensing galaxy. The separation between the two sources (A and B) is $\sim$ 0.3 arcsec.

et al. (2005) with the aim of deriving the Hubble constant from time delay of flux variations and a mass model of the lens. From these F814W images a spiral structure is clearly apparent.

3   SPECTROSCOPY AND DATA ANALYSIS

Observations were obtained on February 2015 at the GTC using the low resolution spectrograph OSIRIS[1] (Cepa et al. 2003). The instrument was configured with the two grisms R1000B and R1000R, in order to cover the spectral range 4000-10000 Å, and with a slit width = 1" yielding a spectral resolution $\lambda/\Delta\lambda = 800$. For each grism three individual exposures were obtained in order to perform optimal cleaning of cosmic rays and of CCD cosmetic defects.

Data reduction was carried out using IRAF[2] and adopting the standard procedures for long slit spectroscopy with bias subtraction, flat fielding, and bad pixel correction. Individual spectra were cleaned of cosmic-ray contamination using the L.A.Cosmic algorithm (van Dokkum 2001). Wavelength calibration was performed using the spectra of Hg, Ar, Ne, and Xe lamps providing an accuracy of 0.1 Å over the whole spectral range. Spectra were corrected for atmospheric extinction using the mean La Palma site extinction table[3]. Relative flux calibration was obtained from the observations of spectro-photometric standard stars secured during the same nights of the target observation. No

---

[1] http://www.gtc.iac.es/instruments/osiris/osiris.php
[2] IRAF (Image Reduction and Analysis Facility) is distributed by the National Optical Astronomy Observatories, which are operated by the Association of Universities for Research in Astronomy, Inc., under cooperative agreement with the National Science Foundation.
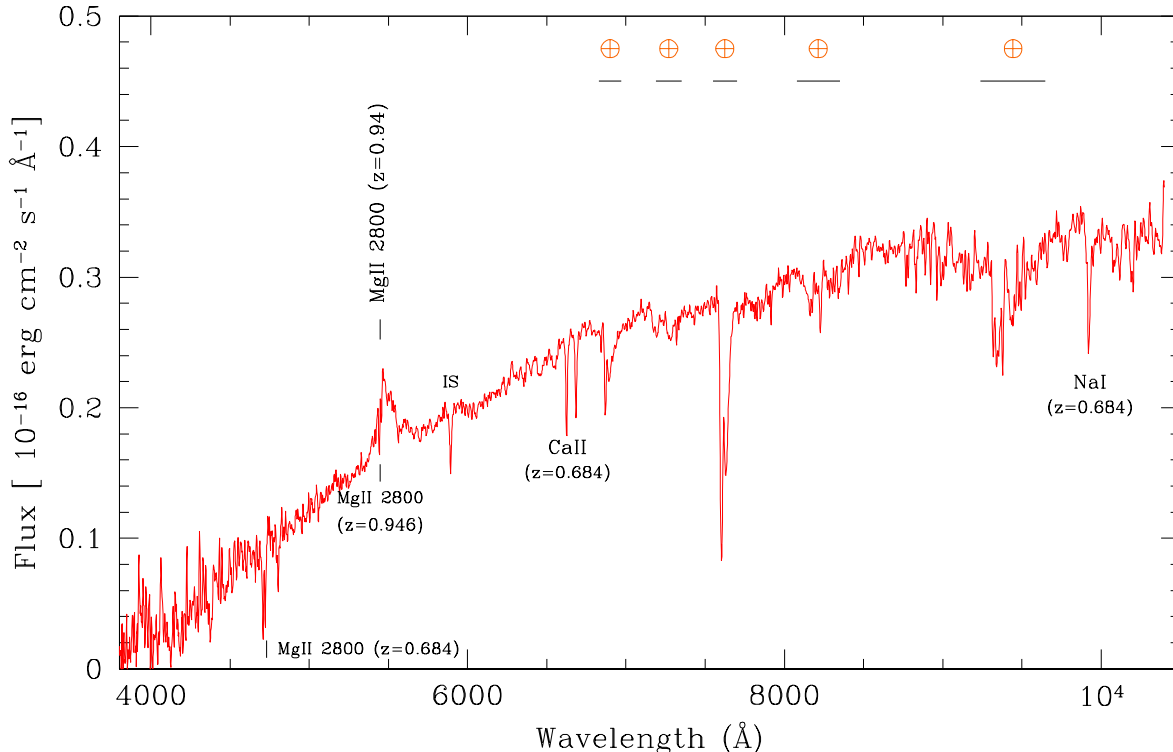[3] https://www.ing.iac.es/Astronomy/observing/manuals/

Figure 2. The optical spectrum of B0218+357 obtained at GTC + OSIRIS. The main absorption features are indicated. The spectral regions affected by telluric absorptions are labelled ⊕. IS marks the galactic interstellar absorption of Na I 5892 Å.

correction for the telluric absorptions was done. The spectra obtained with the two grisms were merged into a final spectrum covering the whole desired spectral range and calibrated to have the flux at 6231 Å equal to the photometry found for the target from a short exposure r band image secured before the spectra. Finally the spectrum was de-reddened for galactic extinction (Cardelli et al. 1989) assuming the E(B-V) = 0.06.

4 RESULTS

4.1 The optical spectrum

Our final optical spectrum (see Figure 2) covers the range between 4000 Å to 10500 Å with a SNR in the range 30-50. The shape of the continuum exhibits a marked decline towards the blue region that is rather unusual for this type of sources and suggestive of a heavy extinction. We confirm the detection of Mg II and Ca II absorption lines at z = 0.684, and in addition we clearly detect an absorption line at 9920 Å that is identified as Na I 5892 Å at the redshift of the lens (see Figure 2 and 3 and Table 1). Contrary to previous spectroscopic results we do not detect the emission lines [OII], H_β and [OIII] reported by Browne et al. (1993) and Cohen et al. (2003). We note that these features are barely detected by these authors and some of them occur inside the telluric absorptions of the O_2 and H_2O. We clearly detect the strong broad emission line at 5480 Å (EW=35 Å, FWHM=4700 km/s) that, assuming it is attributed to Mg

II 2800Å, yields the redshift of z = 0.95 for the blazar. On the blue side of this broad emission line (see Figure 4) there is an absorption doublet of MgII (see Table 1) that is associated with the blazar (Δ V $\sim$ 1000 km/s). We stress that in our spectrum we do not detect the emission lines of H_β and [OIII] at z = 0.95 attributed to the blazar by Cohen et al. (2003). These features are placed in a spectral region heavily contaminated by strong H_2O atmospheric absorption. Therefore we conclude that the redshift is based only on one broad emission line identified with Mg II 2800Å.

4.2 Photometry of B0218+35

In Figure 5 our spectrum is compared to the photometric points derived from the HST images. It is noticeable the very small flux variability of the A and B sources in the HST photometries covering 1995-2000. Comparing the A+B fluxes + galaxy, the photometric agreement is rather good also with our spectrum (Figure 5). Other photometry (e. g. Grundahl & Hjorth (1995), Ahnen et al. (2016), although sparse indicate a modest optical variability of this source as compared to that of other blazars (e.g. Falomo et al. (2014) and references therein).

4.3 Continuum shape and reddening

Blazars emission in the UV-optical band is characterised by a strong non thermal continuum described by a power law
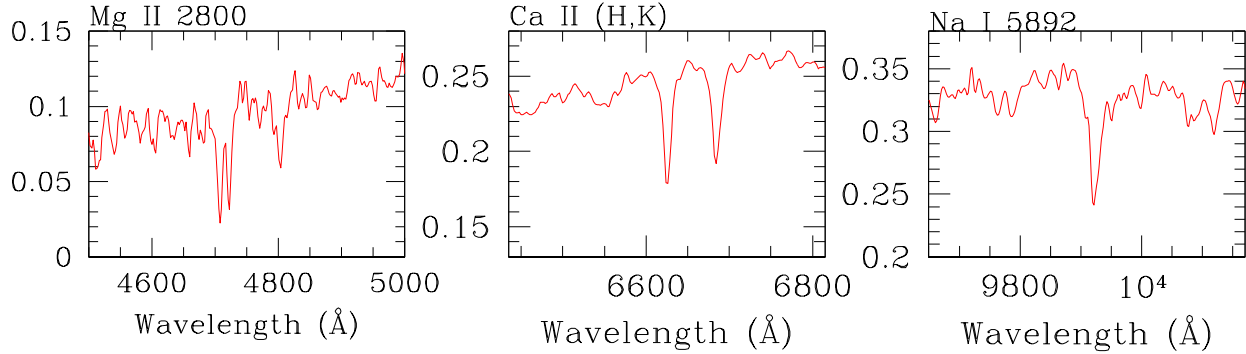
Figure 3. Enlargement of Figure 2 showing the main absorption features in the optical spectrum of B0218+357. Left: MgII 2800, Middle : CaII, Right Na I at the redshift z = 0.684.
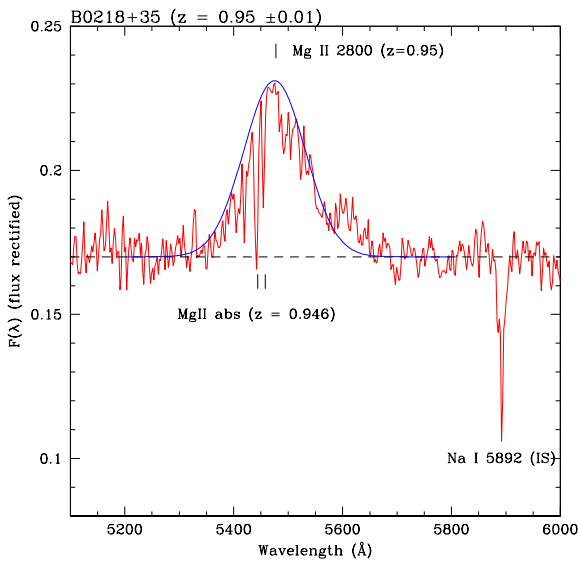

Figure 4. GTC optical spectrum of B0218+357 in the spectral region of the Mg II 2800 broad emission at z = 0.95 ± 0.01. The continuum of the spectrum has been modified to flat shape to better enhance the doublet of Mg II 2800 Å absorption features at z = 0.946.

Figure 5. Optical spectrum of B0218+35 obtained at GTC + OSIRIS compared with the HST photometry (Jackson et al. 2000; Lehár et al. 2000) of the two lensed objects (filled circles) and the total flux (blazar plus lens; open circles). The open triangle represent the aperture photometry of the total light by Grundahl & Hjorth (1995)

($F_\nu \propto \nu^{-\alpha}$) and a thermal component that can be apparent in the UV region (see e.g. Falomo et al. (2014) and references therein). The typical values for α are in the range 0.5-1.5 thus the spectrum is expected to increase towards the blue region (in F_λ units) . The substantial drop of the optical spectrum towards the blue clearly indicates a strong extinction. Since the colours of the two lensed images are
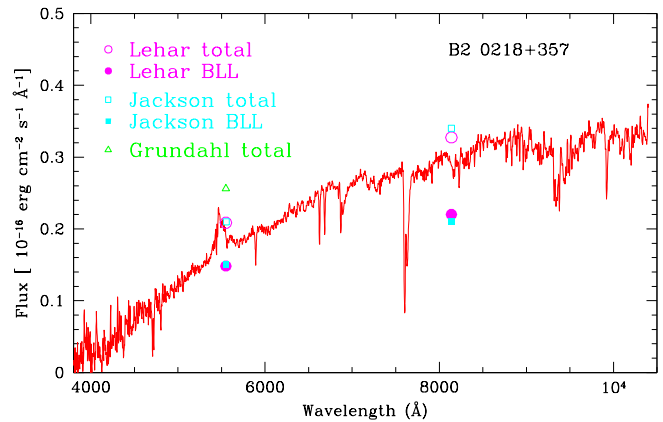
not the same a different extinction for the two light paths was considered.

The subject has been discussed in detail by Falco et al. (1999); Muñoz et al. (2004) who propose a different extinction for A and B and a significant larger value of R_V ($R_V \sim$ 7 and $R_V \sim$ 12) with respect to the galactic one in order to explain the colour difference of the two lensed images in the various bands. The origin of such heavy extinction has been attributed to the lensing galaxy at z =0.684.

From the photometry of HST images (see Sect. 2) the diffuse emission due to the lens galaxy represents a significant fraction of the total observed flux at $\lambda \sim$ 8000 Å . Since our spectrum was obtained with a slit width larger than the diffuse emission we assume that the whole flux from the source (distant blazar and lens galaxy) was gath-

ered. In Figure 6 we compare our optical spectrum with a template spectrum of a late type spiral galaxy (NGC 1057 excluding the prominent emission lines) redshifted at 0.684 and scaled to the flux obtained in the F814W band.

We attempted to fit the observed optical spectrum adding to the galaxy template spectrum the emission of the blazar assuming an intrinsic power law ($F_\nu \propto \nu^\alpha$; $\alpha = -1$) extincted by the absorption in the lens galaxy and assuming both a standard extinction law ($R_V = 3.1$) and higher values of R_V as proposed by Falco et al. (1999); Muñoz et al. (2004). The fit is optimised by changing the value of E_{B-V} and it is normalised to the observed spectrum at $\lambda = 7000$ Å. It turns out that while the spectral region at $\lambda > 6500$ Å can be reproduced adequately, at shorter wavelength a significant excess of emission is found (see Figure 6). In order to compensate for this excess a larger value of E_{B-V} could be invoked but in that case the region at $\lambda > 6500$ Å cannot be satisfactorily reproduced. We also tried to perform the above fit using different values ($-0.5 < \alpha < -1.5$) for the spectral index of the power law emission and the results do not change significantly. The adoption of a different extinction law as that derived for LMC does not help to better reproduce the observations since the main effect is to reduce or avoid the 2175 Å feature in the extinction curve (see e.g. Cardelli et al. (1989)). Under the above assumptions therefore it is not possible to interpret the observed optical spectrum as the combination of a reddened power law and the starlight from a spiral galaxy template.

4.4 Lens galaxy features

From the point of view of the spectral features attributed to the lens galaxy we already noted in Sect. 4 that we do not confirm the detection of emission lines [OII], H_β and [OIII] attributed (Cohen et al. 2003) to the lens galaxy. The only confirmed features are thus the absorptions of Mg II and Ca II (see Table 5). In addition we also detect Na I absorption at the same redshift (see Figure 2, 3 and Table 1). These lines are more likely due to interstellar gas (at z = 0.684) than to the starlight from the lens galaxy. In fact these narrow features do not appear diluted by the non thermal continuum and no other photospheric absorptions (as G band or Mg I 5175) are revealed in our spectrum (see e.g. Figure 6).

Note also that no signature of Ca II break is present. These anomalies were also partially noted by Jackson et al. (2000). The observed spectrum is at most marginally consistent with the presence of a disc galaxy at z= 0.684 assuming the fluxes derived by HST images (see Jackson et al. (2000); Lehár et al. (2000); York et al. (2005)). The redshift derived from K and H absorption lines is : 0.68445 ± 0.00005 that is marginally consistent with that ($z=0.68466 \pm 0.00004$) derived from the 21cm neutral hydrogen transition (Carilli et al. 1993).

4.5 The extinction at z = 0.95

In Sect. 4.3 we showed that the observed optical spectrum cannot be interpreted as a power law plus lens galaxy at z=0.684 with any reasonable value of extinction(E_{B-V} and R_V) The detection of the MgII absorption lines at z=0.946 (see Sect. 4.1) suggests the presence of gas and dust associ-

Table 1: Measurements of the spectral features*

Wavelength (Å)	EW (Å)	Identification	z	
		Blazar		
5440.8	(1.3)	MgII 2795.5	0.946	a
5454.7	(1.0)	MgII 2802.7	0.946	a
5470	∼40	MgII 2800	0.95	e
		Lens galaxy		
4708.0	6	MgII 2795.5	0.684	a
4721.5	5	MgII 2802.7	0.684	a
6625.8	3.5	CaII 3933.6	0.6844	a
6684.7	3.2	CaII 3968.5	0.6844	a
9924.8	6	Na I 5982	0.684	a

Table 1. * Values in parenthesis are uncertain because of the blend with the broad emission. Labels in the last column: a = absorption, e = emission.

ated with the blazar that could produce significant extinction at the source.

In order to reconcile the observed spectrum with a typical non thermal power law emission of the blazar we attempted to fit the data assuming that the main extinction occurs very close to the blazar (at z =0.95). In Figure 7 we report our best fit that assumes $\alpha = -1.5$ and galactic extinction law with $R_V = 3.1$. Under these assumptions we find a significant better fit (weighted RMS 0.016 wrt 0.024) with the data with respect to the case where the absorption occurs at z =0.684.

5 DISCUSSION

5.1 The conventional view

The generally accepted picture for the source B0218+35 is that it is a gravitational lensed blazar, and that the lens galaxy at z = 0.684 coincides with the nebulosity detected in the HST images. The key observations to support this interpretation are the presence of an Einstein ring in the radio (Biggs et al. (2001)) and the radio correlated flux variability (Biggs et al. 2001). There are, however, some difficulties that is worth mentioning here.

a) We do not confirm the alleged redshift for the lens, showing that all confirmed lines are most probably due to intervening absorption gas not necessarily associated to the lens galaxy since no photospheric absorption lines at z= 0.684 are detected. One could argue that for the CaII and NaI lines this is due to the dominance of the gas component, however, one would expect to detect both MgI 5175 Å and G band, which are not observed (see Figure 2). Although we cannot exclude that the intervening gas belongs to the lens galaxy the observed spectrum appears inconsistent with the superposition of a non thermal continuum plus a late type galaxy spectrum at the observed fluxes (see Sect. 4.3)

b) Because of the very small separation (~ 0.3 arcsec) of the two images of the lensed blazar the mass of the lens is expected to be rather small (few times 10^{10} M⊙; Grundahl & Hjorth 1995; Barnacka et al. 2016), in possible tension
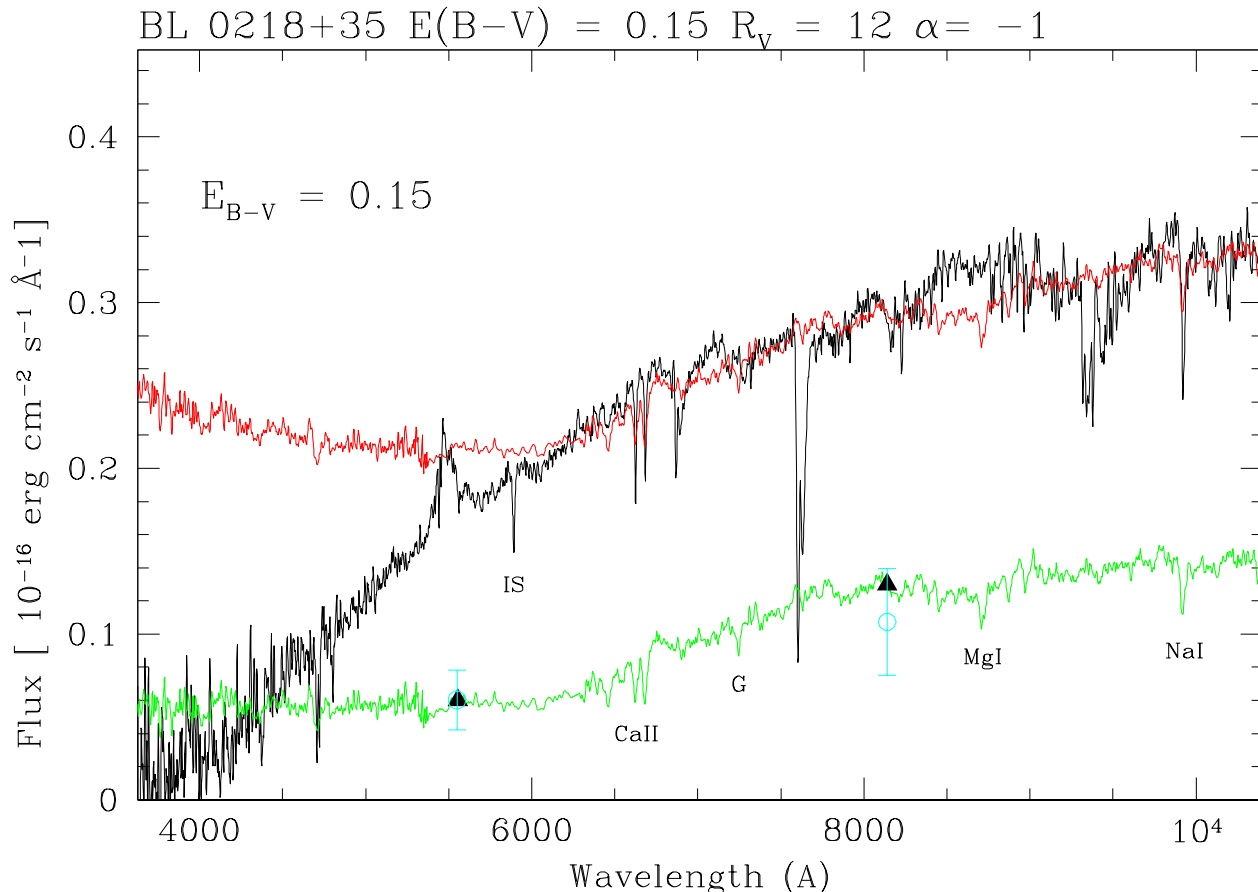
Figure 6. The observed optical spectrum of B0218+35 (black line) compared to a model (red line) obtained adding the spectrum of late type spiral galaxy plus a power law emission ($F_\nu \propto \nu^{-1}$) reddened using an extinction law with $E_{B-V} = 0.15$ assuming $R_V = 12$ as in Muñoz et al. (2004). The spectrum of the template galaxy (NGC 1057 with emission lines removed; green line) has been normalised to the flux given by Jackson et al. (2000) (filled triangles) and by Lehár et al. (2000) (open circles). The fit is remarkably different from the observations in the blue region (see text for details).

with the mass derived from the luminosity ($M(R) \sim -23$) of the lens galaxy estimated from HST images (Lehár et al. 2000; Jackson et al. 2000) assuming a very conservative mass to light ratio M/L =1 . We cannot rule out, however, that only the nuclear region of the galaxy acts as a lens.

c) The shape of the continuum of the lensed source is inconsistent with a typical power law ($F_\nu \propto \nu^\alpha$) spectrum of blazars (see e.g. Falomo et al. 2014, and references therein) assuming an extinction law at the redshift of the lens with large R_V as derived from the color difference of the two lensed images. In Figure 6 we show the comparison between the observed spectrum and that expected assuming it is the combination of a disc galaxy at z=0.684 and a power law emission ($\alpha = -1$) taking an extinction with $R_V = 12$. A substantial difference is apparent at $\lambda < 6000$ Å between the fit and the observed spectrum. The fit becomes even worse if a smaller or a greater value of the spectral index is used (see Figure 8).

5.2   An alternative scenario

Because of the above anomalies we are here considering an alternative scenario of B0218+35. Since neither stellar absorptions nor emission lines are firmly detected at z = 0.684 from the image of the galaxy it is plausible that the nebulosity detected with HST is instead due to the host galaxy of the blazar. Taking z = 0.95, the absolute magnitude then becomes $M_I \sim -24.1$ ($M_R \sim -23.5$) that is consistent with typical host galaxies of QSO. In the optical spectra we detect absorption lines of Mg II 2800 at the redshift (Δ V $\sim$ 1000 km/s) of the blazar. This is suggestive of the presence of gas and dust in the line of sight that is associated to the host galaxy, not the lens. Under these assumptions it is possible to reproduce the observed spectrum with an intrinsic power low emission that is reddened by a standard ($R_V = 3.1$) galactic extinction law (see also Sect. 4.5 and Figure 7). A further improvement of the fit is obtained if one adds an extra extinction at z=0.684, E(B-V) =0.1 and R_V=12 (see Figure 9). In this scenario the non detection of the stellar absorption lines from the host galaxy could be explained since at the redshift of the source (z=0.95) all prominent ones fall
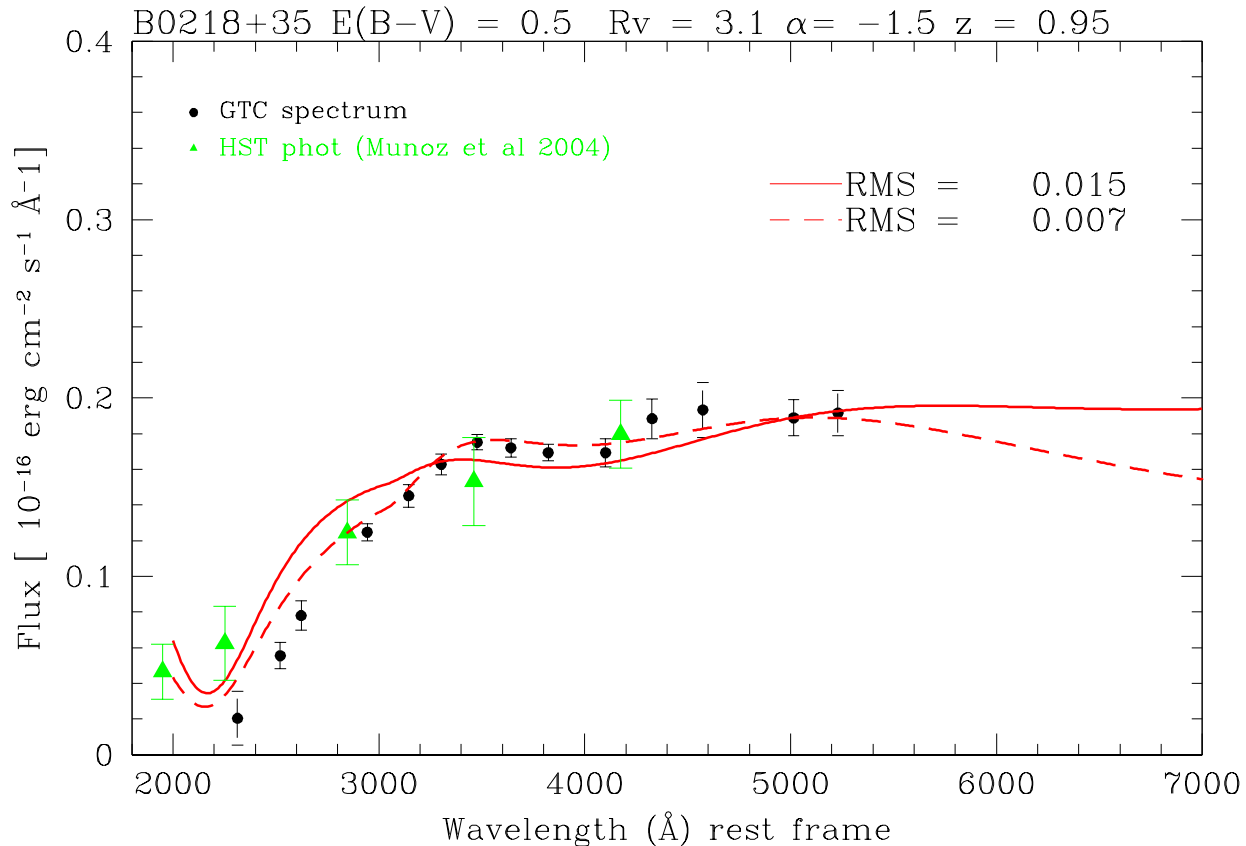
Figure 7. The continuum (black points) at rest frame of the blazar B 0218+357 (z=0.95) is compared to a model of a power law (α = -1.5) extincted (red solid line) using R_V = 3.1 and E(B-V) = 0.5. The optical continuum of the blazar is derived subtracting the contribution of the template galaxy to the observed spectrum (see text for details) that are in good agreement with the HST photometry of the blazar (A+B components; green filled triangles) obtained by Muñoz et al. (2004). The dashed red line represents the fit above (solid red line) with the addition of an extra extinction at z =0.684 and R_V = 12 and E(B-V) = 0.1.

in a region highly affected by the atmospheric absorption bands (e.g. Ca II would be at 7730-40 Å).

The consequences of this picture are :

a) The spectral absorption lines at z=0.684 are due to the halo gas of an intervening galaxy. There are various examples of absorption features in BL Lac objects, that are due to this effect (Landoni et al. 2014; Paiano et al. 2017), and not always the identification of the galaxy is obvious.

b) Apart possibly for its redshift, the properties of the lens galaxy (luminosity and size) remain unknown. The strong absorptions at z=0.684 together with the lack of stellar lines suggest it is a low luminosity gas dominated galaxy, as expected from the small separation of the two gravitationally lensed images. This might imply a substantial revision of the lens models for B0218+357.

c) Under this scenario one would expect that also the image of the host galaxy of the blazar be distorted by the lensing effects. However, since the mass of the lens is likely very small it is not surprising that the distortion be not detectable by the HST images. Moreover the very tiny difference of position ($\sim$ 50 mas) between the centre of the extended nebulosity and of image B, if real, could also be consisted with a low mass lensing galaxy.

6   SUMMARY AND CONCLUSIONS

We presented a new optical ($\lambda\lambda$ 4000–10500 Å) spectrum of the lensed blazar B0218+357 that was recently detected at TeV energies confirming the blazar nature of this source. The analysis of this optical spectrum reveals a number of features that allow us to elucidate some of the puzzling properties of this source and to emphasize peculiarities that suggest possible different interpretation of the system.

From the analysis of our GTC spectrum we confirm the presence of a broad emission line of Mg II 2800 Å yielding a redshift of z = 0.95. However, we contradict the detection of other emission lines claimed by Cohen et al. (2003) thus, although likely the redshift of the blazar is based only on one broad emission feature. On the other hand we confirm the detection of absorption features of Mg II 2800 Å and Ca II (H,K) at the same z and furthermore we detect also Na I 5892 Å absorption at the same redshift. We argue that these lines are arising from interstellar gas likely associated to an intervening galaxy since no other absorption features arising from the stellar population (i.e. G band, MgI 5175 Å) of the lens galaxy are found.

In the field around the target (see Figure 9) there are two galaxies. One (G1) is relatively bright (I $\sim$ 17.8) at 19 arcsec S from the target and another much fainter (I $\sim$ 21.8) at 9 arcsec S. While the former is unlikely to be at the redshift of the intervening absorptions the latter is a plausible
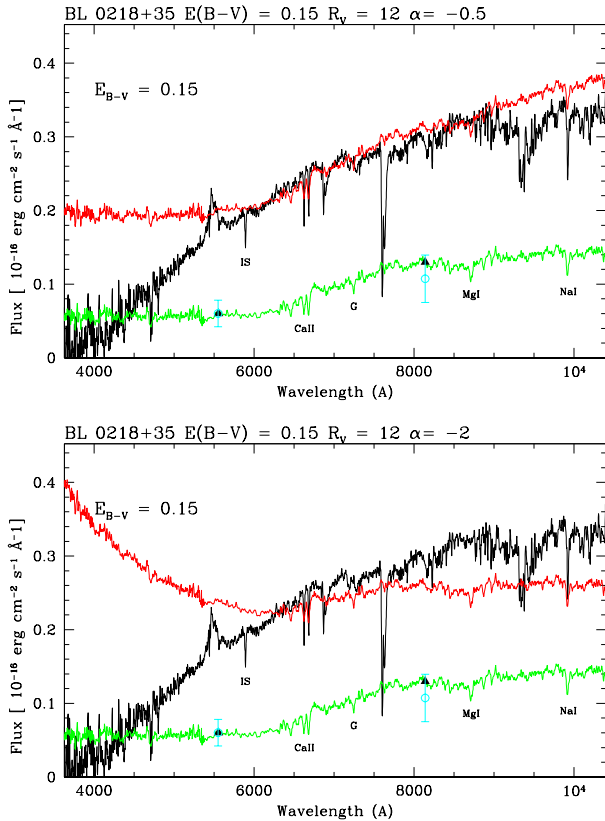
Figure 8. Similar to Figure 6 but using different spectral indices for the power law.
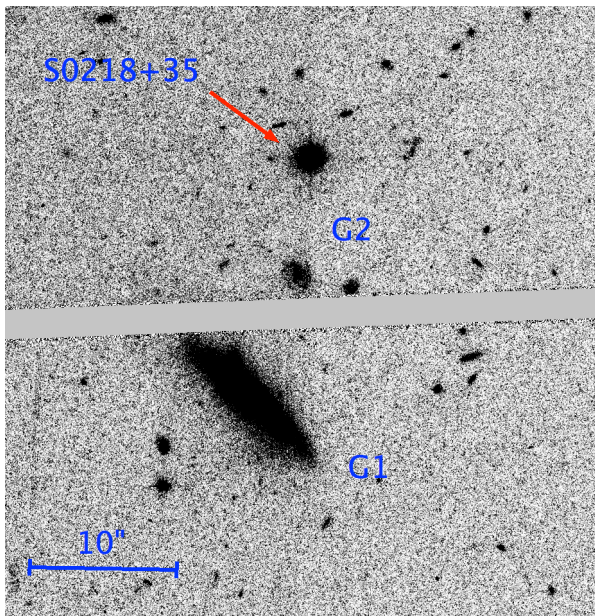

Figure 9. HST ACS image of the field around S0218+35. The target is close to the separation between the two detectors of the WFC. Two nearby galaxies are observed: G1 at 19 arcsec (PD = 130 kpc) and G2 at 9 arcsec (PD = 65 kpc) at z = 0.684. See text for more details.

candidate for the associated intervening absorption. In fact if the galaxy G2 be at z =0.684 then the projected distance from B0218+357 would be only ~ 65 kpc and its absolute magnitude $M_I = -21.8$.

It is apparent that the nature of B0218+357 is still rather puzzling. In order to fully understand the properties of this system spectroscopy of the nebulosity and of the individual A and B sources together with spectra of the galaxies in the immediate environments are mandatory. The detection of stellar spectral lines from the nebulosity would yield unambiguously its redshift. These observations require high sensitivity and adequate angular resolution and are likely achieved in the near future with the new generation of telescopes and instrumentations as JWST, TMT and E-ELT.

REFERENCES

Ahnen, M. L., Ansoldi, S., Antonelli, L. A., et al. 2016, A&A, 595, A98

Barnacka, A., Geller, M. J., Dell'Antonio, I. P., & Zitrin, A. 2016, ApJ, 821, 58

Biggs, A. D., Browne, I. W. A., Muxlow, T. W. B., & Wilkinson, P. N. 2001, MNRAS, 322, 821

Browne, I. W. A., Patnaik, A. R., Walsh, D., & Wilkinson, P. N. 1993, MNRAS, 263, L32

Cardelli, J. A., Clayton, G. C., & Mathis, J. S. 1989, ApJ, 345, 245

Carilli, C. L., Rupen, M. P., & Yanny, B. 1993, ApJ, 412, L59

Cepa, J., Aguiar-Gonzalez, M., Bland-Hawthorn, J., et al. 2003, in , 1739–1749

Cheung, C. C., Larsson, S., Scargle, J. D., et al. 2014, ApJ, 782, L14

Cohen, J. G., Lawrence, C. R., & Blandford, R. D. 2003, ApJ, 583, 67

Falco, E. E., Impey, C. D., Kochanek, C. S., et al. 1999, ApJ, 523, 617

Falomo, R., Pian, E., & Treves, A. 2014, A&A Rev., 22, 73

Giommi, P., Polenta, G., Lähteenmäki, A., et al. 2012, A&A, 541, A160

Grundahl, F., & Hjorth, J. 1995, MNRAS, 275, L67

Jackson, N., Xanthopoulos, E., & Browne, I. W. A. 2000, MNRAS, 311, 389

Landoni, M., Falomo, R., Treves, A., & Sbarufatti, B. 2014, A&A, 570, A126

Lawrence, C. R. 1996, 173, 299

Lehár, J., Falco, E. E., Kochanek, C. S., et al. 2000, ApJ, 536, 584

Muñoz, J. A., Falco, E. E., Kochanek, C. S., McLeod, B. A., & Mediavilla, E. 2004, ApJ, 605, 614

Paiano, S., Landoni, M., Falomo, R., et al. 2017, ApJ, 837, 144

Patnaik, A. R., Browne, I. W. A., King, L. J., et al. 1993, MNRAS, 261, 435

Refsdal, S. 1964, MNRAS, 128, 307

van Dokkum, P. G. 2001, PASP, 113, 1420

Wiklind, T., & Combes, F. 1995, A&A, 299, 382

York, T., Jackson, N., Browne, I. W. A., Wucknitz, O., & Skelton, J. E. 2005, MNRAS, 357, 124